LABORATORI NAZIONALI DI FRASCATI
SIS-Pubblicazioni

LNF-97/026(P)
15 Luglio 1997

ON THE ABSENCE OF MULTIPLE DIPS IN DIFFRACTION OF HIGH ENERGY HADRONS

Małecki and M. Michalec*
*K E N Pedagogical University**, *Cracow, Poland*
and
M. Pallotta
Laboratori Nazionali di Frascati dell' INFN, Frascati, Italy

Abstract

An unorthodox insight into the structure of the geometrical Chou-Yang model explains the experimentally observed paradox of elastic diffraction of high energy hadrons without multiple dips. It is pointed out that the shadow scattering, away from the forward peak, is governed by small values of the coupling strength.

PACS: 13.85.-t, 03.80.+r, 11.80.-m

Submitted to Physical Review D

* Ph.D student at H. Niewodniczański Institute of Nuclear Physics, Kraków.
** Institute of Physics and Computer Science, ul. Podchorążych 2, 30-084 Kraków, Poland; e-mail: AMALECKI@VSB01.IFJ.EDU.PL.

The behaviour of elastic differential cross-section in high energy hadron scattering does not agree with standard ideas about collision of hadrons. In particular, it does not agree with the geometrical models [1,2] of scattering that were supposedly patented to function at high energies. High energy hadron-hadron scattering is strongly absorptive which means that the available energy goes mainly into the production of a very rich set of inelastic final states while the direct two-body channels are suppressed. Yet, as a consequence of unitarity, substantial elastic scattering still takes place through a feed-back from the inelastic channels. This feed-back process is referred to, by analogy to the suppression of the amplitude of light waves by opaque or semi- transparent objects, as shadow or diffraction scattering. According to this optical analogy, diffraction should be associated with multiple dips in elastic differential cross-section. But experiments have, so far, seen no multiple dips. There is hardly any dip in the $p-\bar{p}$ elastic differential cross -section at Tevatron [3] ($\sqrt{s}$=1800 GeV) and SPS collider [4] ($\sqrt{s}$=546,630 GeV) energies while elastic $p-p$ and $p-\bar{p}$ cross-sections at ISR [5] energies ($20 \leq \sqrt{s} \leq$60 GeV) have only one dip. When critically examined, the elastic differential cross-sections of lightest nuclei [6,7] reveal at most one unambigous dip. Taken together, the experimental data constitute a puzzling problem, that is of a diffractive phenomenon which does not have the supposedly well established characteristcs of diffraction, familiar from optics and wave mechanics.

The puzzle would be resolved if there could be diffraction in the sense of unitarity-driven shadow scattering, which is not necessarily accompanied by multiple dips. This is what the experimental data seem unambigously to be suggesting. We claim in this note that this is indeed the case also theoretically. It will be shown that structures in differential cross-sections depend crucially on the effective strength of the interaction governing the scattering process and, correspondingly, on the characteristic length scales involved. Optical-like diffraction with its characteristic forward peak and multiple dip structure is governed by long distance dynamics and large values of the effective coupling strength. Shadow scattering in hadron-hadron collisions at medium and large momentum transfers, on the other hand, is governed by short distance dynamics and small values of the coupling strength.

We reached these conclusions by re-examining geometrical models and studying them as exact mathematical formulations. With this purpose in mind the model parameters are to be free to vary in all possible ways and not only within the bounds allowed by a reasonable fitting to the experimental data. The basic ingredient of the geometrical models is the real, dimensionless opacity function $\Omega(b)$ which depends on a relative impact

parameter b of interacting hadrons and appears in the eikonalized scattering amplitude:

$$T(q) = \frac{i}{(2\pi)^2} \int d^2b e^{i\vec{q}\cdot\vec{b}} T(b); T(b) = 1 - exp[-\Omega(b)], \tag{1}$$

$q = \sqrt{|t|}$ being the momentum transfer in the centre-of-mass system. This amplitude can be reduced, under an implicit assumption of the rotational symmetry of the opacity $\Omega(b)$, to the one-dimensional Bessel transforms of integer order [8]:

$$T(q) = \frac{i}{2\pi} \int_0^\infty dbbJ_0(qb)T(b) = -\frac{i}{2\pi} \int_0^\infty dbb^2 \frac{J_1(qb)}{qb} \frac{dT(b)}{db}. \tag{2}$$

The second form of (2), valid for $T(b)$ vanishing at $b \to \infty$ faster than $b^{-1/2}$, makes it clear that in the geometrical models elastic diffraction takes place mainly at the edge of the absorbing profile $T(b)$.

The optimistic dynamical conjecture was that the opacity can be expressed in terms of hadronic shapes known from other experiments, e.g. in the Chou-Yang model [2] it is assumed that the Fourier transform of $\Omega(b)$ is proportional to the product of the electromagnetic form factors of the colliding hadrons $F_{H_1}(|t|)F_{H_2}(|t|)$. Rather than from experiment, for simplicity of illustration, we take these form factors as the extrapolations to all values of $|t|$ of the asymptotic quark model behaviour:

$$F_H(t) = (1 + \frac{|t|}{m^2})^{1-\nu_H} \tag{3}$$

where ν_H is the number of valence quarks in the hadron H, m being a mass scale parameter. For a pion ($\nu_H = 2$) this gives a single pole form factor and for a proton ($\nu_H = 3$), a dipole. The opacity function then reads

$$\Omega(b) = gh_\nu(mb), h_\nu(mb) = \frac{2}{\Gamma(\nu-3)} (\frac{mb}{2})^{nu-3} K_{\nu-3}(mb) \tag{4}$$

where $g \equiv \Omega(0)$ is a dimensionless coupling parameter, $\nu \equiv \nu_A + \nu_B$ and $K_\nu(mb)$ is the modified Bessel function [8]. For simplicity, the mass scale m in the two hadronic form factors was taken the same.

The predictions of the Chou-Yang model with the opacity (4) are far richer than it had been usually recognised. In its standard phenomenological application [9], the proportionality constant $g(s)$ between the opacity of the hadron and the Fourier transform of the square of its form factor, was simply adjusted to the experimental value of the total cross-section $\sigma_{tot}(s) = 8\pi^2 ImT(s, t = 0)$. But when this experimental constraint is relaxed, one finds that the model can accomodate a surprisingly wide range of behaviour of the elastic differential cross-section $d\sigma(s,t)/dt$. Depending on the value of the coupling constant

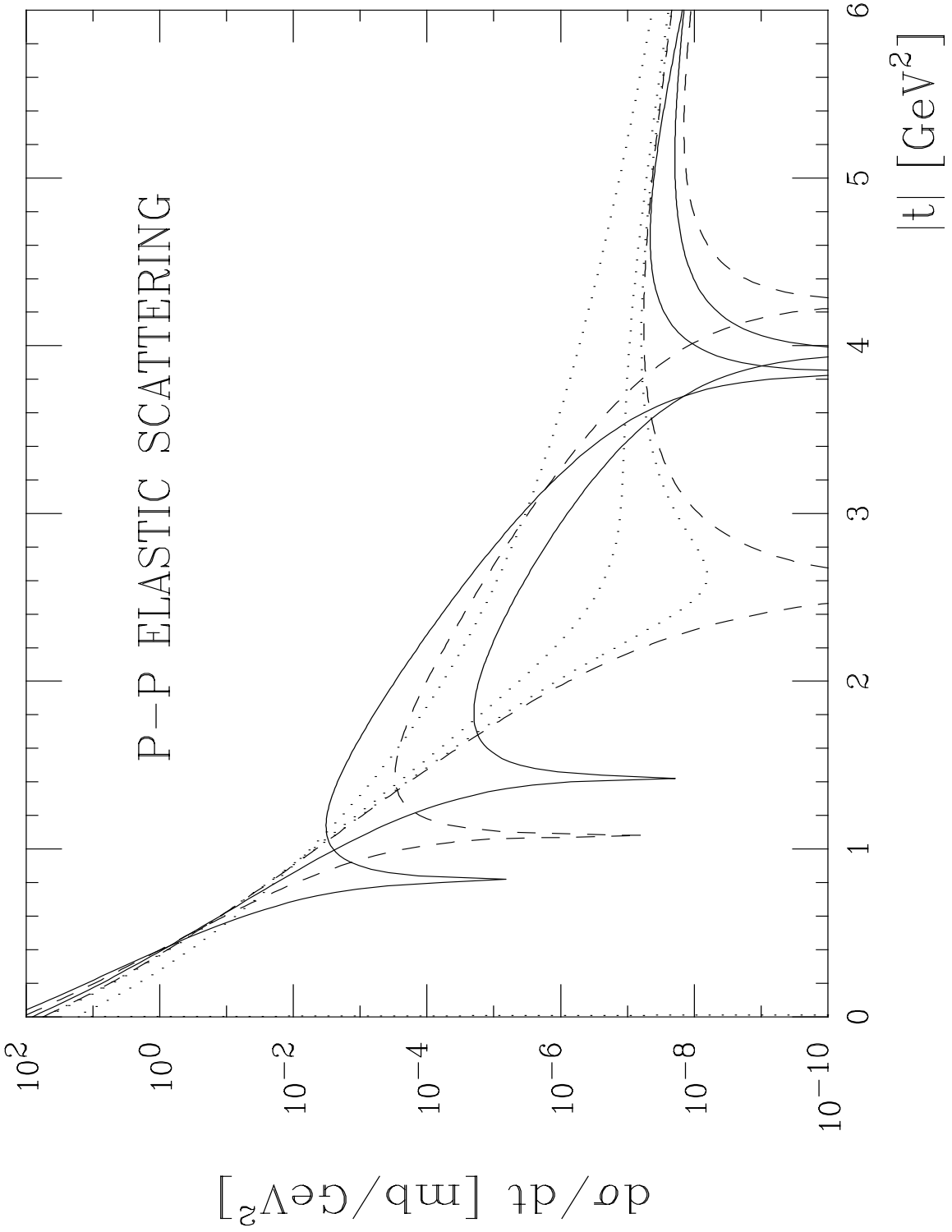

Figure 1: Plots of the elastic differential cross-section for various values of the coupling constant g: 0.50, 0.90, 0.95 (dotted lines), 0.96, 1.50 (dashed lines), 1.20, 2.0 (solid lines). For description - see the text.

g, the $d\sigma(s,t)/dt$ may manifest multiple dips, just one dip (or a single minimum) or no dips (or minima) at all. This is illustrated in Fig.1 where the proton-proton ($\nu = 6$) differential cross-sections are plotted for various values of g and the fixed value of m^2=0.71GeV^2. The coupling constant g acts effectively as a control (or order) parameter. There exists a critical value $g_c = 0.96$ independent of m for which one has just one dip. For small values of the coupling $0 < g \leq 0.50$, the differential cross-section has neither dips nor maxima and minima. A shoulder-like structure that can mimic a minimum appears for some values $< g_c$ (e.g. $g = 0.90$). As g increases towards g_c, the scattering amplitude develops a minimum (e.g. at $g = 0.95$) which gets deeper and deeper becoming a zero of the amplitude. In fact, this zero is a double one. As g increases away from g_c, at once two zeroes appear. The left zero, with increasing g, always moves towards lower values of $|t|$. The right zero, instead, first goes in the opposite direction but when g exceeds the value $g = 1.50$, it turns back and further the two zeroes follow the same way. At another critical value $g = 3.20$ the third zero (also double) appears in the differential cross-section.

It is important to understand how the structures in the elastic differential cross-section arise when the coupling g increases. Qualitatively, it follows from the first form of (2) that since $exp[-\Omega(b)]$ falls off exponentially with g, then large values of g allow for more oscillations of the Bessel function $J_0(qb)$ in the interval $0 \leq b < \infty$. The many oscillations (growing with the momentum transfer q) in the integrand determine the multiple dip structure of the differential cross-section. This dip structure slowly disappears as the effective number of the oscillations is reduced when g decreases. A more quantitative insight into the geometry of elastic diffraction can be gained from studying the derivative of the scattering profile which appears in the second form of (2). We have from (4):

$$\frac{dT(mb)}{d(mb)} = -exp[-\Omega(mb)]\Omega(mb)\frac{K_{\nu-4}(mb)}{K_{nu-3}(mb)}. \qquad (5)$$

These derivative scattering profiles are plotted for various values of g in Fig.2. One observes that the stronger coupling g the closer is the profile $T(g,mb)$ to a sharp-edged absorbing disc. Although the tail of the opacity $\Omega(b)$ at large b is controlled by the mass parameter m, the disc radius and the sharpness of its edge are determined by the coupling g. In fact, the exponential factor in (5) cuts off the low b part of the $\Omega(b)$ distribution, doing this more effectively the greater is the value of g. At the same time, the large value of g induces an increase of the heigth of $\Omega(b)$. In the limit $g \to \infty$ the scattering profile $T(g,mb)$ would approach a step function $\Theta(R-b)$ which corresponds to scattering by a sharp, black disc of radius R. This can also be seen in momentum space upon taking the

limit $g \to \infty$ directly in the first form of the scattering amplitude (2)

$$T(t;g,m) = -\frac{i}{(2\pi)m^2}\int_0^\infty dh \frac{du(h)}{dh} u(h) J_0[\frac{\sqrt{|t|}}{m}u(h)]\Theta(h(0)-h)[1-e^{-gh(u)}], \quad (6)$$

$u(h)$ being the function inverse to the function $h(u) \equiv h_\nu(mb)$. The leading term of the right-hand-side for $g \to \infty$ may be estimated by observing that then $1 - e^{-gh} \approx 1$ for all $h \geq 1/g$. Thus

$$T(t;g,m)_{g\to\infty} \sim \frac{i}{m^2}\int_0^{u(1/g)} du u J_0(\frac{\sqrt{|t|}}{m}u) \quad (7)$$

where $u(1/g)$ is the value of u satisfying $h[u(1/g)] = 1/g$. This means that for large but finite g, $T(t)$ becomes the Airy-like scattering amplitude $RJ_1(qR)/q$ from a sharp absorbing disc of radius $R(g) = u(1/g)/m$.

The number of dips appearing in the differential cross-section depends thus crucially on the strength of the coupling g. Another way of uderstanding this follows from observation that it is the coupling parameter g that governs the decomposition of the scattering amplitude into a series of multiple collisions. In fact, expanding the exponential $exp[-\Omega(b)]$ in Eq. (1) one obtains upon integration over the impact plane the following expression for the S-matrix ($S = 1 + iT$) of elastic scattering [10]:

$$S(q) = e^{\langle n\rangle}\sum_{n=0}^{\infty}(-1)^n P_n \delta^{(2)}(\vec{q} - \vec{q}_n) \quad (8)$$

This formula describes the distribution of all possible partitions of the momentum transfer $\vec{q}$. It is governed by the Poissonian $P_n = e^{-\langle n\rangle}\langle n\rangle^n/n!$ with the mean value $< n >= g$. The terms of the multiple scattering series (8) alternate in sign. Only for very small values of the coupling constant $g \ll 1$ the scattering amplitude is a positive function of the momentum transfer. But for values of g close to unity and larger, this amplitude necessarily has zeroes which give rise to the dips in the differential cross-section.

The coupling g is not the only variable parameter in the Chou-Yang model. There is also the mass scale parameter m in the form factor (3). Having relaxed the condition which fixed $g(s)$ to the experimental value of the total cross-section $\sigma_{tot}(s)$ one can, in the same spirit, let m to be a free parameter. Strict commitment to the fact that $F_H(t)$ should be the electromagnetic form factor extracted from experiments is then not required. There is ambiguity enough, concerning the question which form factor or combination of form factors [11] is to be used in (3), that justifies our attitude. It turns out that the shape of the elastic differential cross-section is independent of the mass scale parameter m. That is, variations in m at fixed g do not change the behaviour of $d\sigma(s,t)/dt$ e.g. from having no dips to one with multiple dips or vice versa. The positions of the dips, of the maxima and minima are, on the other hand, very sensitive to the value of m. As m increases,

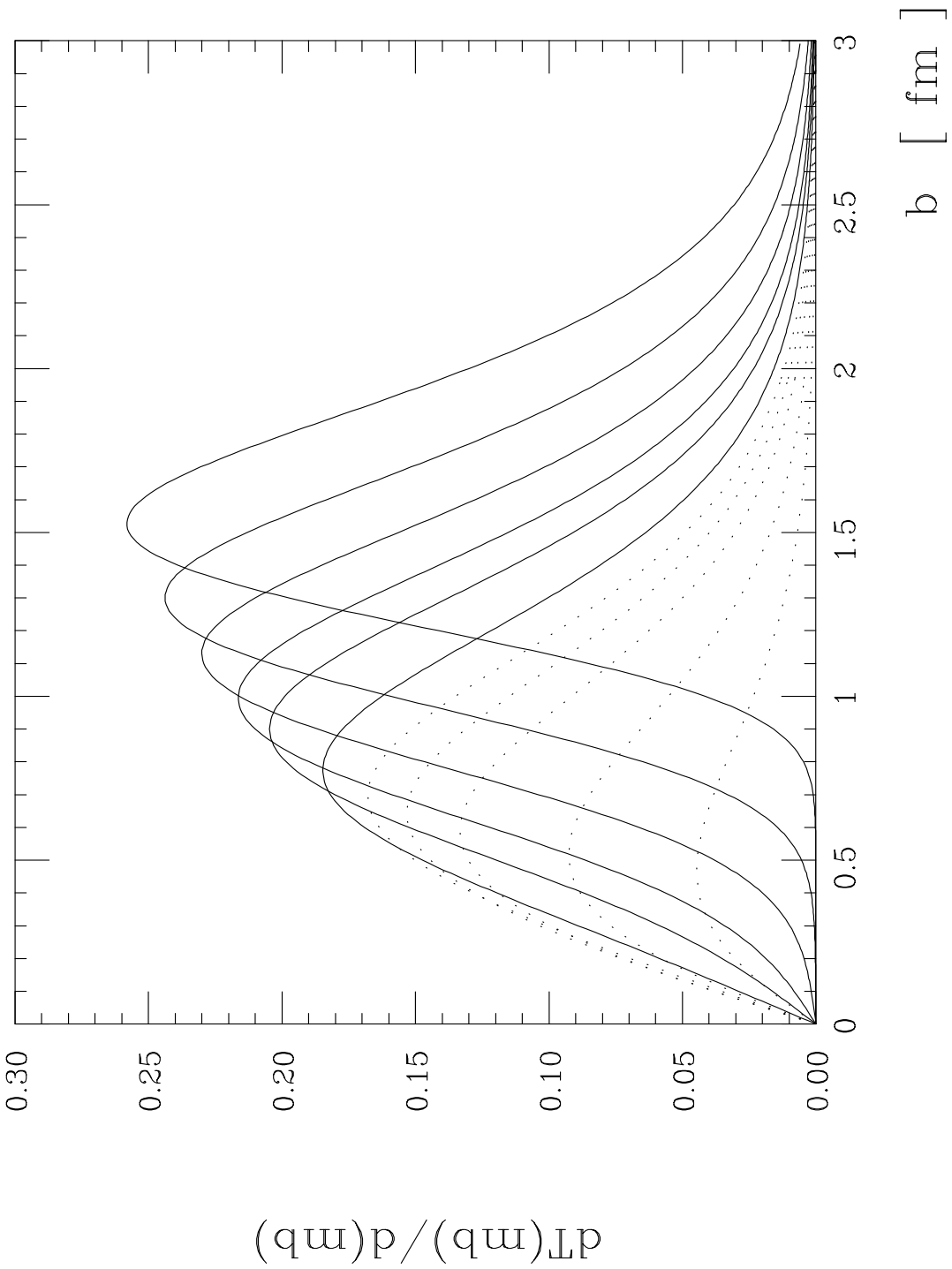

Figure 2: Plots of the derivative of the scattering profile $T(mb; g)$ for various values of the coupling g= 0.2, 0.5, 0.9, 1.2, 1.5 (dotted lines), 2.0, 3.0, 4.0, 6.0, 10.0, 20.0 (solid lines). The greater values of g correspond to larger heigths of the maxima.

these positions move towards the origin ($t = 0$) with a corresponding decrease not only in the value of $d\sigma(s,t)/dt$ but also in the overall value of the integrated elastic cross-section $\sigma_{el}(s)$ and the total cross-section $\sigma_{tot}(s)$. These total cross-sections scale with $m(s)^{-2}$. A value of $m(s) = m_0(s)$ can therefore be found to match the position of the minimum in $d\sigma(s,t)/dt$ with the single dip-like structure in the experimental cross-section. The total cross-section $\sigma_{tot}(s)$, the integrated elastic cross-section $\sigma_{el}(s)$ and the slope parameter $\beta(s)$ of the elastic differential cross-section at $t = 0$, are increasing functions of g but decreasing functions of m. Values of σ_{tot} in the range of the experimental ones (e.g. in $p-p$ and $p-\bar{p}$ at ISR and SPS energies) correspond to values of $g(s) > g_c$ and, therefore, to multiple dips in $d\sigma(s,t)/dt$. They correspond too to values of $m(s) < m_0(s)$ and hence to positions of the single dip-like structure in $d\sigma(s,t)/dt$ far away from the experimental one. It is, therefore, not possible to reconcile the experimental values of $\sigma_{tot}(s)$, $\sigma_{el}(s)$ and $\beta(s)$ with the absence of mltiple dips in $d\sigma(s,t)/dt$ and with the position of its single dip-like structure in the model. Adjusting $g(s)$ around g_c to get the experimental shape of $d\sigma(s,t)/dt$ and $m(s)$ around $m_0(s)$ to get the position of the single dip produces a value of $d\sigma(s,t)$ many orders of magnitude smaller than the experimental one. The experimental values of $\sigma_{tot}(s)$,$\sigma_{el}(s)$, $\beta(s)$, on the one hand, and the shape and structure of $d\sigma(s,t)/dt$, on the other, constitute therefore rather severe constraints, particularly because getting the one tends to ruin the other.

Despite of the failure in fitting experimental data the Chou-Yang model has, as we have seen earlier, other and profounder merits. The model does not predict only multiple dips, characteristic of familiar optical diffraction. It has an astonishing virtue of accomodating all kinds of behaviour of the elastic differential cross-section. The coupling constant g of the model is much more than just a fit parameter. If the appearance of dips is interpreted as a classical-like phenomenon, then g operates as a kind of geometrical size parameter in a way remarkably similar to the inverse of Planck's constant $\hbar$. This is reminiscent of the rôle of $\hbar$ in semiclassical approximations to quantum scattering on which geometrical models are essentially based. Thus $g \to \infty$ corresponds to large distances in much the same way as $\hbar \to 0$ corresponds to a classical macroscopic regime.

We would like to point out that geometrical models have been used, so far, only in this 'macroscopic' limit giving rise to optical-like diffraction with its characteristic multiple dip structure. In fact, the basic assumption of these models is that the incident particle is way out of the target before the effects which it induces in the latter take place. This means that the projectile hadron sees the target, essentially , as a geometrical obstacle of given finite size. In other words, the geometrical models, as usually applied, include an implicit assumption of asymptotic sharp-edged disc (black or grey) scattering at large distances.

On the other hand, a lot was gained simply by the knowledge how the limit $g \to 0$ operates in the Chou-Yang model. This limit corresponds to $\hbar \to \infty$, which means a regime where quantum effects are not at all negligible. More than just classical wave-like properties could emerge in such a limit. In this 'submicroscopic' limit the absorbing disc scattering, operative at large distances, will be replaced by point-like scattering at short distances, i.e. inside the geometrical obstacle. It appears clearly from our previous discussion that diffraction in high energy hadron-hadron collisions, understood as a unitarity driven shadow scattering, would rather be influenced (away from the forward peak) by short distance dynamics connected to small values of the coupling strength. This prompt us a useful distinction between two sources of elastic diffraction: the geometrical diffraction on an absorbing hadronic bulk, considered as a shadow of non-diffractive transitions, and the short-range dynamical diffraction, appearing as the unitarity effect from intermediate diffractive transitions. Such a two-component model was constructed by one of us in a recent publication [12] and applied succsessfully to elastic scattering and inclusive inelastic diffraction of high energy hadrons.

This communication resulted from our collaboration with Dr. E. Etim. His contribution is gratefully acknowledged. This work was partially supported by the Polish Committee for Scientific Research (K B N) and the Italian Institute for Nuclear Physics (I N F N).

References

[1] R. J. Glauber, in **Lectures in Theoretical Physics**, ed. by W. E. Brittin and L. G. Dunham (Interscience, New York, 1959), vol.1, p.315; R. J. Glauber and J. Velasco, Phys.Lett. **B 147** (1984) 380.

[2] T. T. Chou and C. N. Yang, Phys.Rev. **170**(1968)1591, Phys.Rev. **D 19** (1979) 3268.

[3] E-710 Collab., N.A.Amos et al., Phys. Lett. **B 247** (1990) 127.

[4] UA4 Colab., M.Bozzo et al., Phys.Lett. **B 155** (1985) 117; D. Bernard et al., Phys.Lett. **B 171** (1986) 142.

[5] K.R. Schubert, Tables of nucleon-nucleon scattering, in: **Landolt-Börnstein, Numerical data and functional relationship in science and technology**, New Series, Vol.1/9a (1979); A. Breakstone et al., Nucl.Phys. **B 171** (1986) 142.

[6] L. Satta et al., Phys.Lett. **B 139** (1984) 263.

[7] A. Małecki, Phys.Rev. **C 44** (1991) R1273.

[8] M. Abramowitz and I. A. Stegun, **Handbook of Mathematical Functions**, Dover Publications, New York, p. 355.

[9] F. Hayot and U. P. Sukhatme, Phys.Rev. **D 10** (1974) 2183.

[10] E. Etim, A. Małecki and M. Pallotta, **LNF-94/046 (1994)**.

[11] E. Leader, U. Maor, P.G. Williams and J. Kasman, Phys.Rev. **D 14** (1976) 755.

[12] A. Małecki , Phys.Rev. **D 54** (1996) 3180.